The fabrication process of polydimethylsiloxane (PDMS) nanostructured films with antimicrobial properties against methicillin-resistant *staphylococcus aureus* (MRSA)

N. L. M. Shamsuddin, K. Mohamed*
Nanofabrication and Functional Materials (NFM) Research Group, School of Mechanical Engineering, Engineering Campus, Universiti Sains Malaysia, 14300 Nibong Tebal, Penang, Malaysia

Physical topography modification is an approach to fabricate nanostructures surfaces with antimicrobial properties. Lithography-based technologies offer an effective technique to develop the desired sizes and geometry. The replica molding technique was employed to fabricate the PDMS nanostructures using the PMMA imaging layer and characterized using a FESEM and AFM. The cell viability of gram-positive bacteria on structural diminished by almost 80% and the cells were deformed and ruptured once attached to the structured surface. Thus, the PDMS structured surface enhanced the bactericidal properties of the film, which effectively inhibit bacterial attachment.

(Received October 17, 2023; February 28, 2024)

Keywords: Nanostructure, Lithography, PDMS, PMMA/Si, Antimicrobial properties

1. Introduction

The discovery of naturally occurring nanostructured surfaces has been reported to exhibit significant bactericidal activity against pathogenic elements. For example, the surface of dragonfly (*Orthetrum villosovittatum*) and cicada wings (*Psaltoda claripennis*) are able to repel and rupture the cell wall of several pathogenic bacterial strains upon attachment, including that of *Bacillus subtilis*, *Escherichia coli,* and *Pseudomonas aeruginosa* [1,2]. The surface of dragonfly wings, which were found to have nanostructure dimension of about 200 – 300 nm in height, 60–100 nm in diameter, and 150–210 nm in pitch size, showed substantial impact against the growth of both gram-negative and gram-positive bacteria[3]. Additionally, previous studies have revealed that naturally occurring nanostructured surfaces exhibit other unique functions, such as self-cleaning mechanism, superhydrophobic, and anti-biofouling properties[4–8]. It was reported that the cicada wing surfaces consist of an array of spherically-capped, conical nanoscale pillars with periodic hexagonal position[2].

The antimicrobial properties of nanostructured surfaces are due to the mechanical stretching, dimensional, and penetration effects between the bacterial cells and the surface features. The recent findings of such fascinating naturally occurring surfaces have inspired researchers to fabricate artificial nanostructured surfaces that mimic the unique properties that found in nature for various biological applications. Numerous research groups have published comprehensive reviews of the proposed nano-architectures for antimicrobial surfaces based on these biological features[9–11].

Lithography is one of the reliable techniques for the fabrication of nanostructured surfaces. The structures fabricated via lithographic techniques can be designed with regular arrays and controllable dimensions. Numerous studies have evaluated the antimicrobial activities of nanostructured surfaces subjected to the design and geometric effects. Table 1 shows the application of various lithography techniques to fabricate nanostructure surfaces with bactericidal properties by other research works. It was suggested that a higher number of nanostructures on the developed surface would increase the contact with the bacterial cell, thus, enhancing the bactericidal properties.

* Corresponding author: mekhairudin@usm.my
https://doi.org/10.15251/DJNB.2024.191.325

This suggestion was supported by Hazell *et al.*[12] through the fabrication of polyethylene terephthalate (PET) nanocone structure arrays with 200 nm and 500 nm spacing using the colloidal lithography technique. The result showed significant dead bacterial cells that were attached to the PET nanocone surface compared to that on the controlled flat surface. The finding was in agreement with the works by Wu and co-workers[13], Kelleher *et al.*[8], and Dickson *et al.*[14], which also reported higher bactericidal activity using denser nanostructured surfaces. Hence, the antimicrobial response not only depends on the topographic characteristics of the surface, such as the contact angle, surface roughness, and surface energy, but also the dimensions of the features, including the aspect-ratio, geometry, height, tip pitch size, pitch spacing, and density of nanostructure, as well as the properties of the microbial cell itself[15].

Table 1. Fabrication of micro/nanostructured surfaces using various lithography techniques.

Surface	Features	Technique	Bactericidal efficacy
Ormostamp nanopillar[13]	Diameter ~80 nm Average density ~40 pillars/μm^2	UV-NIL	Effective against *S. aureus*
Polyethylene terephthalate (PET) nanocone[12]	Base diameter of 55–381 nm Tip width of 20–304 nm Height of 352–529 nm	Colloidal lithography	Effective against *E. coli* and *Klebsiella pneumoniae*
Moth-eye nanopillar/PET film[16]	Pitch of 200 nm Height of 200 nm	UV-NIL	Effective against *S. aureus* and *E. coli*
Polymethyl methacrylate (PMMA) nanopillar[14]	Diameter of 70–215 nm Height of 200–300 nm	NIL	Lethal effect against *E. coli*
PMMA nanopores film[17]	Depth of 460 nm Spacing of 300 nm Aspect ratio of 3.0	Thermal NIL	Restricted attachment of *P. aeruginosa* and *E. coli*
Polyurethane Sharklet micropattern[18]	Height of 3 μm Width of 2 μm Spacing of 2 μm	Thermal embossing	Lethal effect against *Staphylococcus epidermidis* and *S. aureus*

One such productive lithography method is the Electron Beam Lithography (EBL) that can be utilised to fabricate a master mold with a high-resolution patterning capability down to a few nanometres in size. This molding technique has several advantages over other methods for the transfer of patterns, including straightforward, ease of fabrication, and not being subject to a diffraction limitation. The fabricated master mold can be employed multiple times, thus, reducing the cost and time involved in the fabrication process. The capability to fabricate highly precise nanostructures on a diverse range of materials is essential to biological applications. Polydimethylsiloxane (PDMS), which is a biocompatible, optically transparent, low toxicity, and elastomeric polymeric material, can also be used to transfer nanostructured patterns for many biomedical applications, for example, implant, microfluidic, catheters, and contact lenses.

The gram-positive Methicillin-resistant *Staphylococcus aureus* (MRSA) are selected in this study since early studies reported that nanostructured surfaces were less effective against gram-positive bacteria due to their peptidoglycan layer that is 4–5 times thicker compared to that in gram-negative bacteria[2,5]. This strain commonly associated with skin infections or contamination of surgical wounds, bloodstream, lungs, and urinary tract.

To date, several fabricated nanostructured surfaces, such as black silicon[19,20], titania[21], or titanium nanowires[22] and polymer[13], have shown promising bactericidal properties against both gram-positive and gram-negative bacterial strains. Therefore, this study was performed to investigate the fabrication process of nanostructured PDMS films with antimicrobial properties. Using the EBL technique, the proposed topographic surface was fabricated on a developed master mold. Subsequently, the pattern was transferred onto the PDMS surface via the replica molding (soft lithography) technique. Following the surface characteristic analysis, the MRSA strain was used as the bacterial inoculum to assess the bactericidal activity on the fabricated PDMS surfaces.

2. Methodology

2.2. Fabrication of the PDMS nanostructure film

The overall fabrication process of the PDMS nanostructured film is shown in Fig. 1. Firstly, the master mold was produced as follows: The 1 cm^2 cleaned silicon was spun-coated with polymethyl methacrylate (PMMA) with a molecular weight of 996k (Sigma Aldrich) in 3 wt% chlorobenzene (Sigma Aldrich) at 4000 rpm for 60 s. The PMMA/Si thin film was pre-baked at temperature 140 ˚C for 30 min in an oven to remove excess solvent. Next, the nanohole pattern array was exposed using a Scanning Electron Microscope (JOEL JSM 6460-LV) system integrated with an EBL (Raith ELPHY Quantum) system to define the pattern as master mold. The EBL exposure was conducted at 200 μm^2 of write field size, 300X magnification, and 0.2 pC of single-pixel e-beam at a working distance of 10 mm. The maximum accelerating voltage of 30 keV was applied to minimise the undesired proximity effect during the e-beam exposure. Following the exposure step, the samples were soaked in a developer solution comprising methyl isobutyl ketone (MIBK):isopropyl alcohol (IPA) at a ratio of 1:3 for 40 s at temperature 23 °C before being immersed in an IPA stopper solution to terminate the pattern developing process. In the final processing step, the mold was rinsed with deionised water and blow-dried with nitrogen gas before being post-baked at temperature 90 °C for 30 min.

The PDMS films were prepared using a PDMS elastomer Sylgard 184 (Dow Corning) mixed with a curing agent at a ratio of 10:1. The mixture was stirred for 5 min before being degassed in a vacuum chamber to remove the trapped air bubbles. Once the mixture was poured onto the mold with an approximate thickness of 2 mm, the thin film sample was degassed again before undergoing the curing process in the oven at temperature 50 °C for 3 hrs. Finally, the cured PDMS film was carefully peeled off from the mold and ready for further analysis.

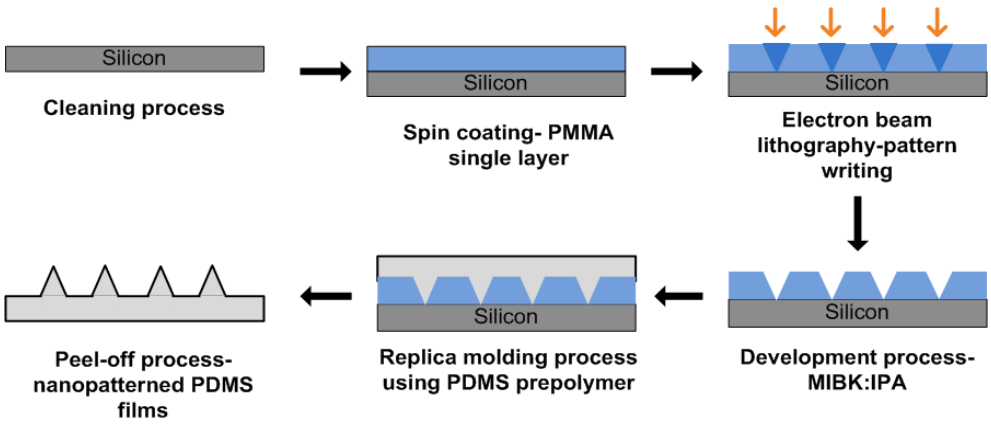

Fig. 1. The schematic fabrication process of the PDMS nanostructured film using the PMMA/Si master mold.

2.3. Bacterial Culture and Viable Plate Count Method

Methicillin-resistant *Staphylococcus aureus* (MRSA) (ACTT 43300) was activated by streaking the strain from the glycerol stock on a Nutrient Agar (NA) plate (Himedia) using a sterilised inoculating loop. The NA plate was incubated for 24 hrs at temperature 37 ºC in an incubator. A single colony from the NA plate was then inoculated into a Nutrient Broth (NB) (Himedia) in an incubating shaker at 120 rpm for 24 hrs and at temperature 37 ºC. The overnight bacterial culture was then suspended in a fresh NB and the concentration was adjusted to 1.0 McFarland standard, which corresponds to approximately 10^8 Colony Forming Units (CFU)/mL. The resuspended bacterial cell was diluted 1000 times in phosphate-buffered saline (PBS). The cell viability assessment was carried out via the standard plate count method[23].

The triplicate PDMS films were loaded into a 6-well plate and seeded with the diluted suspension of MRSA. Then, 1 mL of cell suspension from each well was collected at various incubation periods (3, 6, and 24 hrs) and diluted up to ten-fold in NB. Subsequently, 100 µL of each diluted sample was cultured onto the NA plates using the spread plate method and incubated at temperature 37 ºC in triplicate for each resuspension. After 24 hrs, the colonies on the agar plates were counted and the number of colonies (CFU/mL) was calculated. The CFU value was assumed to be equivalent to the number of living cells in the suspension.

2.4. Surface characterisation of the master mold and PDMS nanostructure

The surface morphology of the PMMA master mold and the PDMS nanostructured film were characterised using a Field Emission Scanning Electron Microscopy (FESEM) (FEI Nova NanoSEM 450). Prior to the FESEM imaging, the sample surface was coated with a thin layer of platinum (Quorum Q150R thin-film coater) as a conductive layer. The surface topography was also analysed using an Atomic Force Microscopy (AFM) (Dimension Edge, Bruker). The instrument was set to the tapping-mode imaging perpendicular to the axis of the cantilever at a frequency scan rate of 1 Hz, 256 points collected per line (pixel resolution), scan size of 10 µm, and analysed with a NanoScope analysis software. The topographic imaging scans were performed using antimony (n)- doped silicon probes (MPP-11100-10; Veeco/Bruker) with a spring constant of 20–80 N/m, tips with a radius curvature of 8 nm, and a resonance frequency between 311 and 361 kHz.

The adhesion of the MRSA cells on the PDMS nanostructured film was analysed as follows. After a 24-hr incubation, the PDMS films were rinsed with PBS twice at room temperature to remove non-adherent bacteria. The samples were then fixed with McDowell Trump's 4F:1G fixative (containing formaldehyde and glutaraldehyde in PBS) for 15 min to suppress chemical reactions due to the bacterial death. The samples were rinsed again with PBS and immersed twice in a series of ethanol at concentrations of 60%, 70%, 80%, 90%, and 100% for 10 min each. The samples were left to dry overnight in the incubator. Prior to the FESEM analysis, the sample was coated with a thin layer of platinum and grounded with a conductive tape. The observation elevation angle was set at 45º and magnification at 2 kX.

3. Results and discussion

3.1. The characterisation of master mold and PDMS nanostructure

The surface morphology and cross-sectional profiles of the hexagonally-arranged nanohole array were observed through the AFM imaging, as shown in Fig. 2. A single-pixel e-beam exposure was utilised during the pattern definition process on the PMMA/Si substrate. The e-beam was exposed onto the PMMA photoresist, which underwent chain scission and soluble fragments when soaked in the developer solution. The penetration depth was approximately 80 nm, as illustrated in Fig. 2(c). In addition, it was observed that lower developing times produced unexposed patterning with undefined shapes. On the contrary, longer developing times resulted in an uncontrolled increase of the width. The e-beam dosage also affected the width and depth of penetration on the PMMA, which led to the formation of well-defined features that are consistent with those reported in other study[24]. The size of the nanohole greatly expanded due to the unstable beam and the influence of electron scattering during the e-beam exposure process. The electrons experienced a small-angle forward scattering upon bombardment onto the surface of the resist, thereby widening the primary beam size during the beam exposure[25]. Subsequently, a large-angle backscattering occurred after the e-beam passed through the resist and penetrates the substrate. In addition, undesirable proximity effects also broadened the effective exposure area in the resist, thereby affecting the targeted feature size.

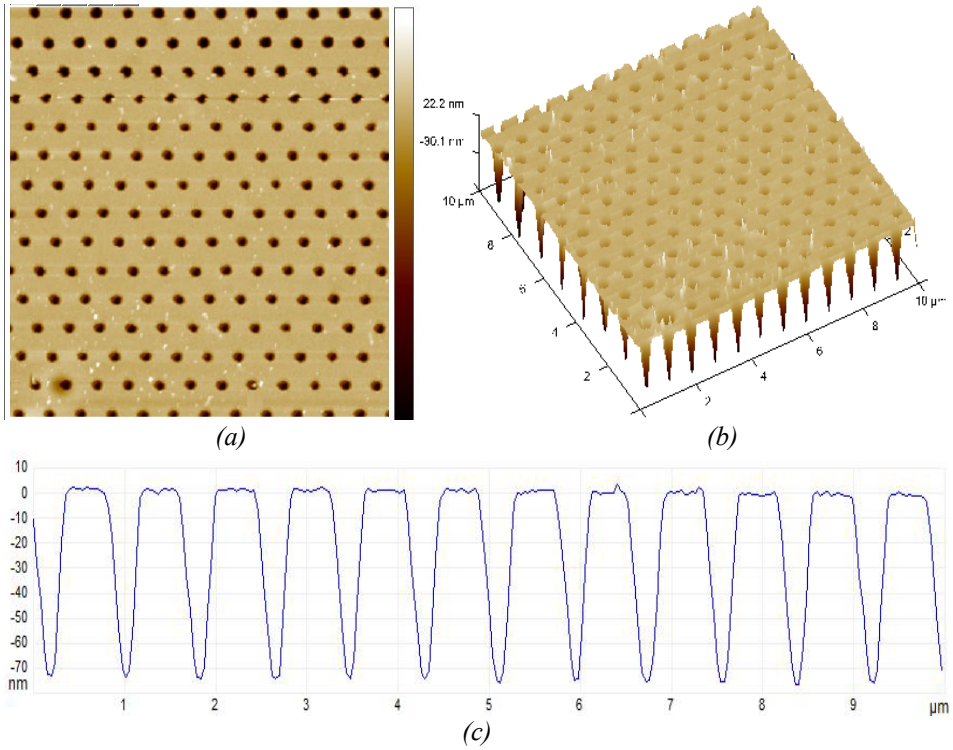

Fig. 2. The surface morphology and cross-sectional profiles of the nanohole array on the PMMA/Si master mold.

The flat surface and three associated PDMS imprint films of the PMMA/Si master mold are presented in Fig. 3. The flat PDMS surface possess the lowest surface roughness of 0.0542 nm (Fig, 3(a)). In comparison, the PDMS nanostructured surface (S1) shown in Fig. 3(b) has a diameter of 308 nm, a height of 160 nm, a pitch distance of 470 nm, and higher surface roughness of 42.4 nm. Meanwhile, the features dimension of S2 in Fig. 3(c) includes a diameter of 220 nm, less half-height compared to S1, spacing between structures of 473 nm, and surface roughness of 26.1 nm. Interestingly, Fig. 3(d) illustrates the structure of S3 with a diameter of 268 nm, pitch distance of 515 nm, height average of 30 nm, and the lowest surface roughness of 12.2 nm. The height differences between the fabricated PDMS nanostructures significantly affected the surface roughness.

Based on the morphological comparison with the master mold, it was evident that the exquisite features of the hexagonally shaped dotted arrays of the master mold surface were successfully replicated onto the PDMS film at a low curing temperature. Previous studies have reported that lower curing temperatures and longer curing times were identified as the ideal conditions to effectively replicate PDMS nanostructures[26,27]. However, the height of the PDMS structure was doubled or elongated compared to that of the cavity depth on the master mold. The deformation of the PDMS nanostructure might be due to the low modulus of PDMS[28]. The root means square (RMS) surface roughness value of the fabricated PDMS surface was extracted and measured from the AFM imaging using the NanoScope analysis software since the fabricated PDMS nanostructures used in antimicrobial MRSA studies vary in features dimensions. The cross-sectional profiles of the PDMS nanostructured surfaces are illustrated in Fig. 3(e).

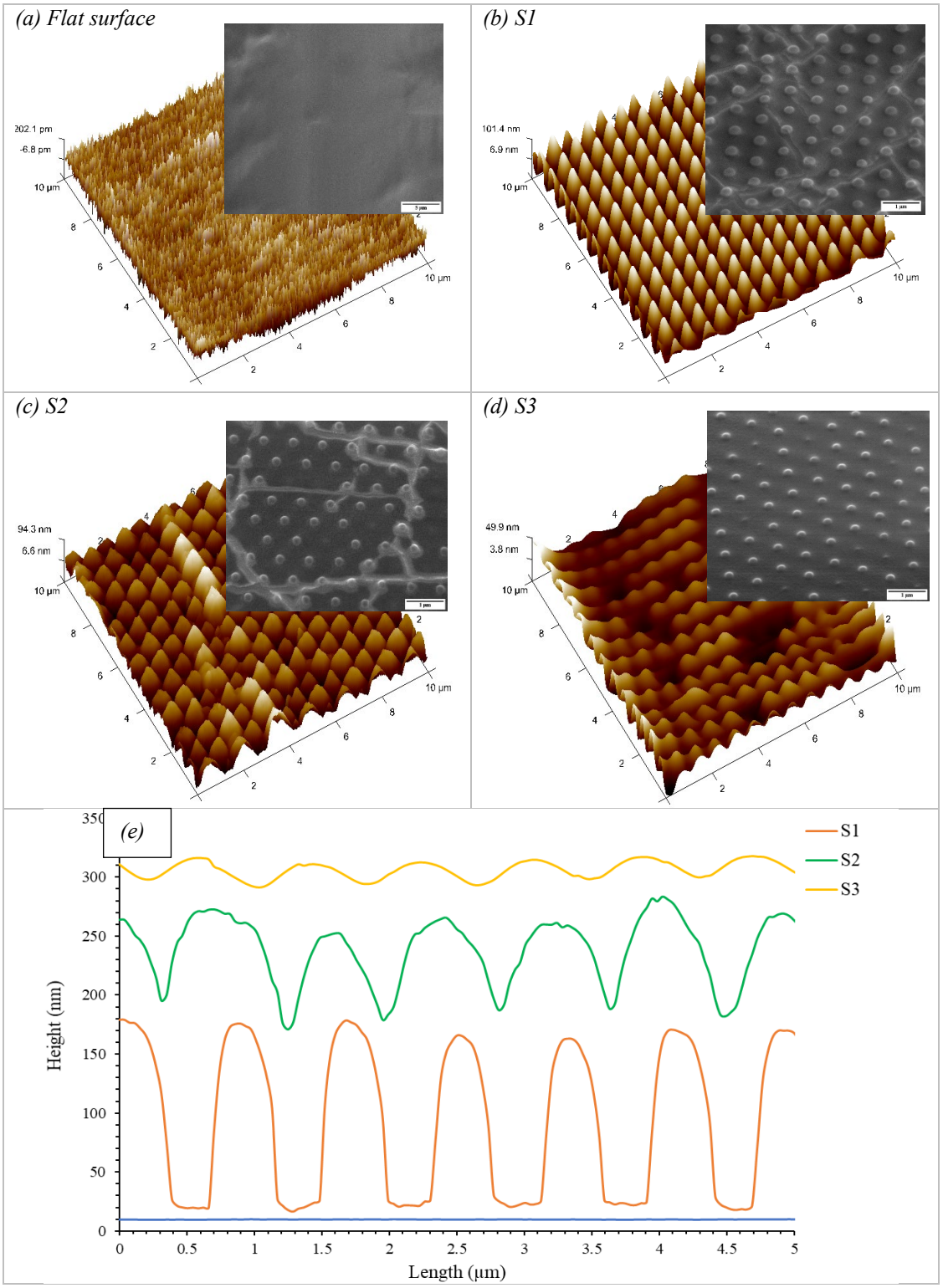

Fig. 3. The AFM topography and FESEM images of (a) flat surface and (b-d) nanostructured surface of the PDMS films. (e) The cross-sectional profile of the flat and PDMS nanostructured surfaces.

3.2. Antimicrobial activity of the PDMS nanostructured film

The bacterial suspension loaded onto the PDMS film was determined after 3, 6, and 24 hrs of incubation periods. Based on the viable cell assessment via the spread plate technique, the countable colonies on the PDMS nanostructured film were less compared to that on the flat PDMS films after 24 hrs of incubation, as shown in Fig, 4. The decreased CFU count over the course of

24 hrs incubation indicated the effective antimicrobial properties of the PDMS nanostructured films in inhibiting bacterial growth compared with the flat PDMS surface [14].

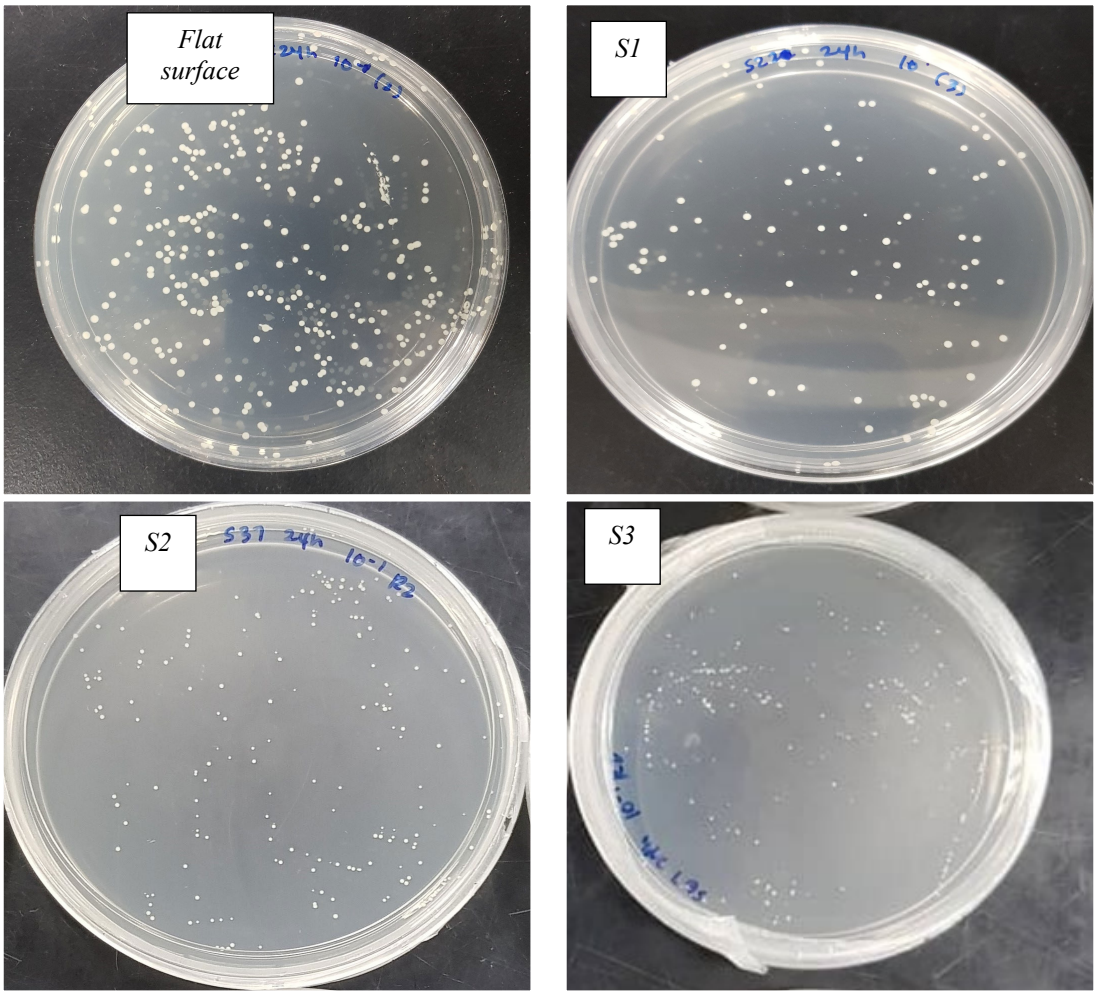

Fig, 4. The optical micrograph of MRSA colonies on the NA plates from the flat and nanostructured PDMS surfaces after 24 hrs of incubation.

Fig, 5 shows the viable bacterial cell count after 3, 6, and 24 hrs incubation periods from the well-plate of each bacterial cell suspension. The viable cell count from the flat PDMS surface is slightly increased by 9% from 3-hrs to 6-hrs before being significantly reduced to 1.06×10^4 CFU/mL after 24 hrs. The count drops might be due to the increased attachment of bacterial cells on the flat PDMS surface compared to the cells that remain suspended in the solution. In contrast, the number of bacterial cells loaded on the PDMS nanostructured film gradually decreased from the beginning of the incubation period. After 24 hrs, the growth of the MRSA in S1, S2, and S3 were 8.76×10^3 CFU/mL, 1.16×10^4 CFU/mL, and 1.33×10^4 CFU/mL, respectively. Note that the colony count in S1 diminished almost 50% after 6 hrs and 80% after 24 hrs. The findings indicate that the PDMS features of S1 with a height dimension of 160 nm resulted in the lowest number of colonies compared to other films with lower overall height dimensions. The obtained results correspond to that in prior studies, which stated that the bactericidal properties depend on the surface topographical features[8].

Fig, 6 shows the FESEM images of the adhered MRSA cells on the flat and patterned PDMS films. A higher number of bacterial cells was observed to adhere on the surface of the flat PDMS compared to that of the PDMS nanostructured surface under the same microscopic magnification. It was assumed that the topographic characteristics of the PDMS surface reduce the

bacterial attachment. Apart from exhibiting the highest structural height, the fabricated nanostructures in S1 possessed a large width area of approximately 300 nm, which induced the hydrophobic properties of the polystyrene film, therefore, minimising the available surface area of the structured polymer surfaces for bacterial attachment [29].

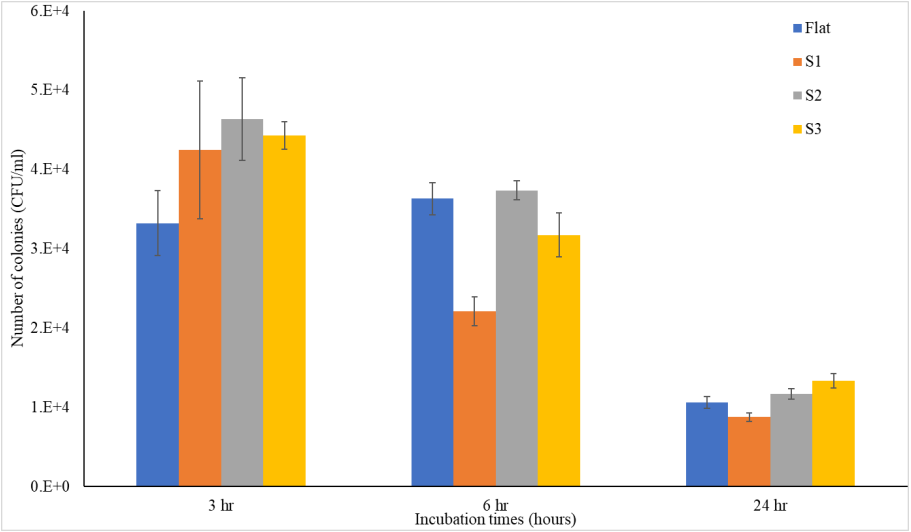

Fig, 5. The viable cell count for flat and nanostructured PDMS surfaces after 3, 6, and 24 hrs of incubation.

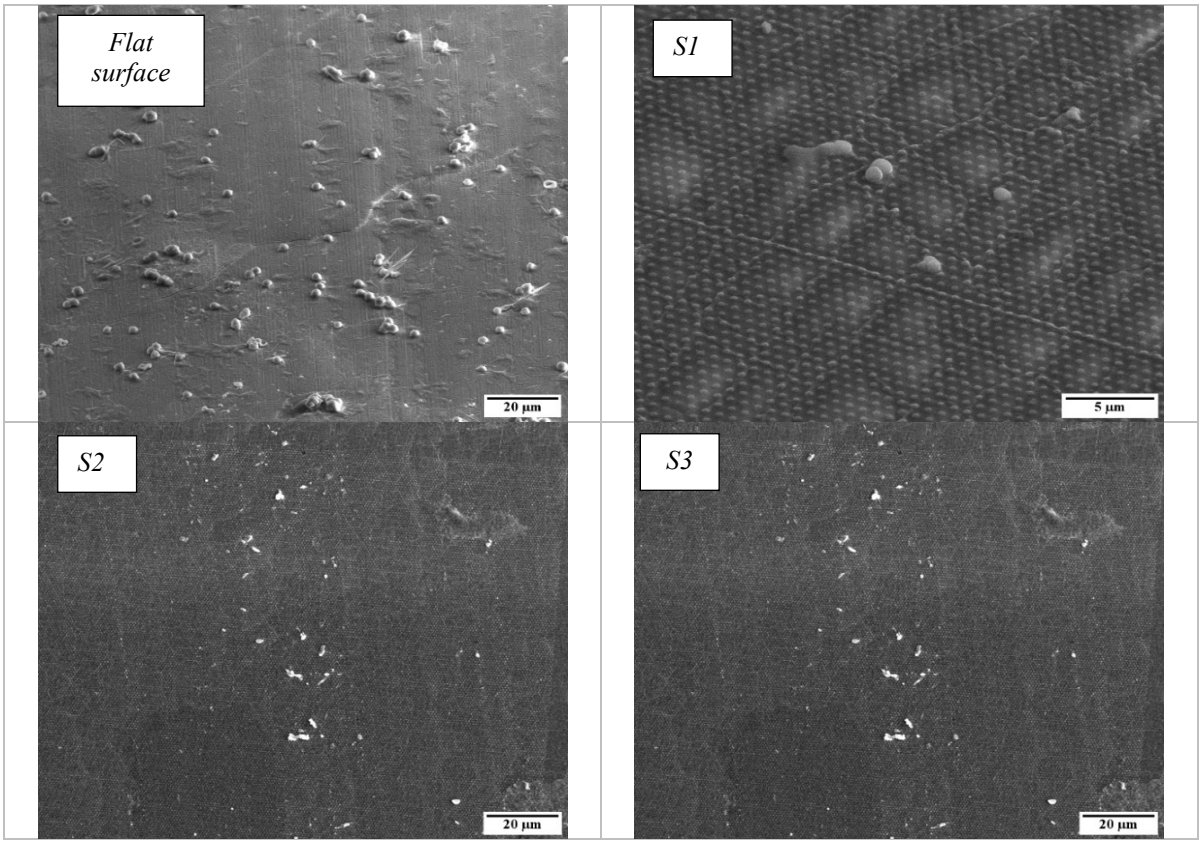

Fig, 6. The FESEM images of MRSA cells on the flat and nanostructured PDMS films.

Fig. 7 shows a closer observation of the MRSA cells that appeared to be deflated on the PDMS nanostructured surface. The interaction between the nanostructures and bacterial cells facilitates the rupture of the bacterial membrane, leading to the imminent death of the cells. Although some bacteria were still able to survive by adjusting their shape and bending the arrays within the surface structure[30], the formation of irregular lumpy bacteria on the nanostructured surface demonstrates that the cells were damaged and ruptured. While previous studies have reported the ineffective action of nanostructured surfaces against gram-positive bacteria due to their thicker peptidoglycan layer, the findings in this study have highlighted the significant bactericidal properties of the PDMS nanostructured surface against the gram-positive MRSA cells. The different dimensions of the patterned surface inhibited most of the bacterial attachment, while those that were able to adhere were severely distorted and failed to proliferate.

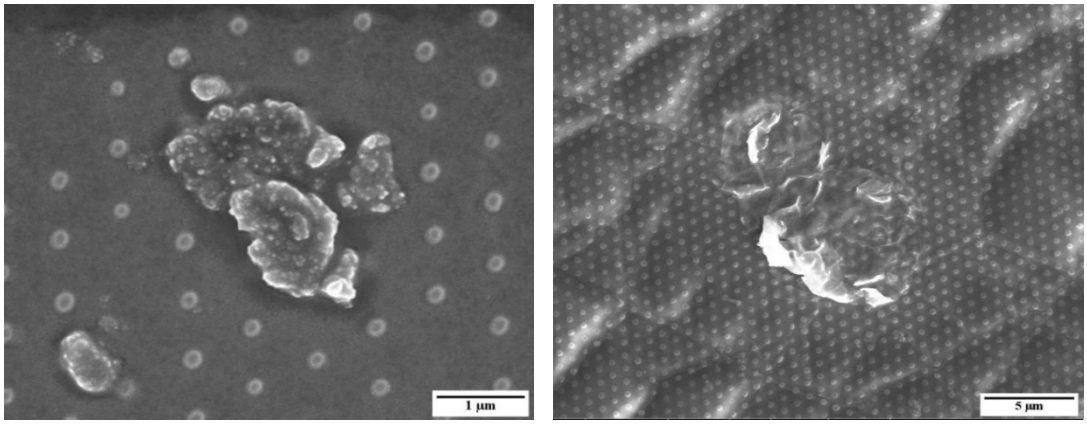

Fig. 7. The ruptured bacteria cells on the PDMS nanostructured surface at (left) 10kX and (right) 50kX magnification.

Table 2 lists the summary of the surface features of S1, S2, and S3 and their corresponding percentage of bacterial reduction (bactericidal efficiency). The PDMS surface with the highest structure height (S1) recorded almost 80% of bactericidal efficiency compared to S2 (75%), S3 (70%), and the flat PDMS surface (68%). The low bacterial cell count on the flat PDMS surface could be due to the increased attachment of bacterial cells to the surface. Furthermore, the higher values of surface roughness of nanostructure (S1) strongly influenced bacterial adhesion[31], which inversely reduced the bactericidal properties of the flat PDMS surface.

Table 2. The topographic features and bactericidal efficiency of the PDMS nanostructured surfaces.

Sample	*Structure diameter (nm)*	*Structure height (nm)*	*Structure spacing (nm)*	*Surface roughness*	*Bactericidal efficiency (%)*
Flat	-	-	-	*0.0542 nm*	*68*
S1	*308*	*160*	*470*	*42.4 nm*	*80*
S2	*220*	*70*	*473*	*26.1 nm*	*75*
S3	*260*	*30*	*515*	*12.2 nm*	*70*

4. Conclusion

The present study demonstrated the successful fabrication process of the PDMS nanostructured surface via the EBL technique with effective antimicrobial properties against gram-positive MRSA cells. The replica molding (soft lithography) was effectively employed as a simple method to replicate the hexagonally shaped dotted arrays of the PMMA/Si master mold onto the

PDMS film at a low curing temperature. The AFM cross-sectional profiles showed the enhanced topographic features of the fabricated PDMS nanostructured surface. Furthermore, the viable cell assessment indicated that sample S1 recorded the highest bactericidal efficiency of up to 80% after 24 hrs of incubation due to its highest structural height and large width area. The bactericidal properties of the PDMS nanostructured surface were highly influenced by the surface roughness and height of the fabricated PDMS films. The different dimensions of the patterned surface also inhibited most of the bacterial attachment, while those that were able to adhere were severely distorted and failed to proliferate. Thus, the feature dimensions affected the ability of the fabricated surfaces to prevent bacterial adhesion and distort the cell structure once attached to the surface.

Acknowledgments

The authors would like to thank the staff and technicians of Institute of Nano Optoelectronics Research and Technology (INOR) School of Physics and School of Biological Sciences, Universiti Sains Malaysia (USM) for providing the facilities for the fabrication and characterisation of the PDMS nanostructures. The authors are also grateful to the Ministry of Higher Education of Malaysia and the School of Mechanical Engineering, USM, for funding the scholarship.

References

[1] C. D. Bandara, S. Singh, I. O. Afara, A. Wolff, T. Tesfamichael, K. Ostrikov, A. Oloyede, ACS Appl. Mater. Interfaces 9, 6746 (2017); https://doi.org/10.1021/acsami.6b13666

[2] E. P. Ivanova, J. Hasan,H.K. Webb, V. K. Truong, G. S. Watson, J. A. Watson, V. A. Baulin, S. Pogodin, J.Y. Wang, M. J. Tobin, C. Löbbe, R. J. Crawford, Small 8, 2489 (2012); https://doi.org/10.1002/smll.201200528

[3] D. E. Mainwaring, S. H. Nguyen, H. Webb, T. Jakubov, M. Tobin, R. N. Lamb, A. H. F. Wu, R. Marchant, R. J. Crawford, E. P. Ivanova, Nanoscale 8, 6527(2016); https://doi.org/10.1039/C5NR08542J

[4] S. Pogodin, J. Hasan, V. A. Baulin, H. K. Webb, V. K. Truong, T. H. P.Nguyen, V. Boshkovikj, C. J. Fluke, G. S. Watson, J. A.Watson, R. J Crawford, E. P Ivanova, Biophys. J. 104, 835 (2013); https://doi.org/10.1016/j.bpj.2012.12.046

[5] J. Hasan, H. K Webb, V. K.Truong, S.,Pogodin, V. A Baulin, G. S. Watson, J. A. Watson, R. J Crawford, E. P Ivanova, Appl. Microbiol. Biotechnol. 97, 9257(2013); https://doi.org/10.1007/s00253-012-4628-5

[6] C. Zeiger I. C. R. da Silva, M. Mail, M. N. Kavalenka, W.Barthlott, H. Hölscher, Bioinspir. Biomim. 11, (2016); https://doi.org/10.1088/1748-3190/11/5/056003

[7] F. Xue, J. Liu, L. Guo, L. Zhang, Q. J. Li, Theor. Biol. 385, 1(2015); https://doi.org/10.1016/j.jtbi.2015.08.011

[8] S. M. Kelleher, O. Habimana, J. Lawler, B. O' Reilly, S. Daniels, E., Casey, A. Cowley, ACS Appl. Mater. Interfaces 8, 14966 (2016); https://doi.org/10.1021/acsami.5b08309

[9] A. Elbourne, R. J. Crawford, E. P. Ivanova, J. Colloid Interface Sci. 508, 603(2017); https://doi.org/10.1016/j.jcis.2017.07.021

[10] J. Hasan, A. Roy, K. Chatterjee, P. K. D. V.Yarlagadda, ACS Biomater. Sci. Eng. 5, 3139 (2019); https://doi.org/10.1021/acsbiomaterials.9b00217

[11] E, A. Cuello, L. E. Mulko, C. A. Barbero, D. F. Acevedo, E. I.Yslas, E. I. Colloids Surfaces B Biointerfaces 188, 110801 (2020); https://doi.org/10.1016/j.colsurfb.2020.110801

[12] G. Hazell, L. E. Fisher, W. A., Murray, A. H., Nobbs, B. J. Su, Colloid Interface Sci. 528, 389 (2018); https://doi.org/10.1016/j.jcis.2018.05.096

[13] S. Wu, F. Zuber, K. Maniura-Weber, J. Brugger, Q. J. Ren, Nanobiotechnology 16, 20 (2018)

[14] M. N. Dickson, E. I. Liang, L. A. Rodriguez, N. Vollereaux, A. F. Yee, A. F. Biointerphases 10, 21010 (2015); https://doi.org/10.1116/1.4922157

[15] A. Tripathy, P. Sen, B. Su, W. H. Briscoe, Adv. Colloid Interface Sci. 248, 85 (2017); https://doi.org/10.1016/j.cis.2017.07.030

[16] K. Minoura, M. Yamada, T. Mizoguchi, T. Kaneko, K. Nishiyama, M. Ozminskyj, T. Koshizuka, I. Wada, T. Suzutani, PLoS One 12, e0185366 (2017); https://doi.org/10.1371/journal.pone.0185366

[17] S. Kim, U. T. Jung, S. K. Kim, J. H. Lee, H. S. Choi, C. S. Kim, M. Y. Jeong, ACS Appl. Mater. Interfaces 7, 326 (2015); https://doi.org/10.1021/am506254r

[18] R. M. May, C. M. Magin, E. E. Mann, M. C. Drinker, J. C., Fraser, C. A. Siedlecki, A. B. Brennan, S. T. Reddy, Clin. Transl. Med. 4, (2015).

[19] E. P. Ivanova, J. Hasan, H. K. Webb, G. Gervinskas, S. Juodkazis, V. K. Truong, A. H. F. Wu, R. N. Lamb, V. A. Baulin, G. S. Watson, J. A. Watson, D. E. Mainwaring, R. J. Crawford, Nat. Commun. 4, 2838 (2013); https://doi.org/10.1038/ncomms3838

[20] J. Hasan, S.Raj, L. Yadav, K. Chatterjee, RSC Adv. 5, 44953 (2015); https://doi.org/10.1039/C5RA05206H

[21] T. Diu, N. Faruqui, T. Sjöström, B. Lamarre, H. F. Jenkinson, B. Su, M. G. Ryadnov, Sci. Rep. 4, 1 (2014); https://doi.org/10.1038/srep07122

[22] C. M. Bhadra, V. Khanh Truong, V. T. H. Pham, M. Al Kobaisi, G. Seniutinas, J. Y. Wang, S. Juodkazis, R. J. Crawford, E. P. Ivanova, Sci. Rep. 5, 16817 (2015); https://doi.org/10.1038/srep16817

[23] J. R. Postgate, Methods in Microbiology, Academic Press vol. 1, 611 (1969); https://doi.org/10.1016/S0580-9517(08)70149-1

[24] A. Veroli, F. Mura, M. Balucani, R. Caminiti, AIP Conf. Proc. 1749, 20010 (2016).

[25] C. S. Wu, Y. Makiuchi, C. Chii Dong, Lithography 656 (2010).

[26] X. Ye, H. Liu, Y. Ding, H. Li, B. Lu, Microelectron. Eng. 86, 310 (2009); https://doi.org/10.1016/j.mee.2008.10.011

[27] D. Hlúbiková, A. T. Luis, V. Vaché, L. Ector, L. Hoffmann, P. J. Choquet, Micromechanics Microengineering 22, 115019 (2012); https://doi.org/10.1088/0960-1317/22/11/115019

[28] K. Mohamed, N. Kooy, K. Ibrahim, Int. J. Nanotechnol. 11, 520 (2014); https://doi.org/10.1504/IJNT.2014.060573

[29] D. Patil, A. Sharma, S. Aravindan, P. V. Rao, Micro Nano Lett. 14, 191 (2019); https://doi.org/10.1049/mnl.2018.5462

[30] S. Mo, B. Mehrjou, K. Tang, H. Wang, K. Huo, A. M. Qasim, G. Wang, P. K. Chu, Chem. Eng. J. 123736 (2019).

[31] A. Chebolu, B. Laha, M. Ghosh, Nagahanumaiah, Micro Nano Lett. 8, 280 (2013); https://doi.org/10.1049/mnl.2013.0109